Frontiers in Heat and Mass Transfer (FHMT), 18, 35 (2022)
DOI: 10.5098/hmt.18.35

Global Digital Central
ISSN: 2151-8629

Frontiers in Heat and Mass Transfer

Available at www.ThermalFluidsCentral.org

LAMINAR FLOW HEAT TRANSFER IN HELICAL OVAL-TWISTED TUBE FOR HEAT EXCHANGER APPLICATIONS

Scott Wahlquist [a], Amir Ali [a,b,*], Su-Jong Yoon [c], Piyush Sabharwall [c]

[a] *Idaho State University, Pocatello, Idaho, 83209, USA*
[b] *Center for Advanced Energy Studies (CAES), Idaho Falls, Idaho, 83401, USA*
[c] *Idaho National Laboratory, Idaho Falls, Idaho, 83415, USA*

ABSTRACT

The heat transfer performance of a novel tube configuration that combines the swirling velocity induced by oval-twisting and secondary flow generated by a helical geometrical flow path is presented. The Nusselt number (Nu) and friction factor (f) are compared for the laminar flow regime (Re = 250-2000) under isothermal wall conditions. Under the same flow and boundary conditions, the oval-twisted helical tube increased the Nu and slightly increased the f over the circular helical tube. The best performance with the highest Nu and lowest f occurs at the coil curvature ratio (d_h/D) of 0.17. The quantified enhancement performance factor (η) shows a 46 - 56% increase for the oval-twisted helical tube over the circular helical tube with d_h/D = 0.17. Correlations for the Nu and f are developed and agreed with the numerical results: ± 6% and ± 5% for the Nu and f, respectively.

Keywords: O*val-twisted, helical tube, advanced heat exchangers, vorticity, enhancement performance factor*

1. INTRODUCTION

The enhancement in heat and mass transfer has become a significant interest for many engineering applications, including heat exchangers (HX). Numerous researchers focused on investigating diverse enhancement techniques to improve performance and increase the compactness of the HX to meet the rising energy and efficiency needs in industrial applications and processes. Mainly, heat transfer intensification techniques for HX are classified under two major categories, namely active and passive (Kurnia *et al.*, 2020). Active methods involve using external power to drive the enhancement mechanism by applying a magnetic or electric field, mechanical mixer and agitator, and vibration. Passive enhancements are achieved through combinations of surface and/or geometrical modifications, aiming to extend/enhance the heat transfer surface area, increase the flow swirling, and strengthen the secondary flow (e.g., changing surface roughness/coatings, extending surfaces/fins, inserting twisted-tape, bending, and twisting). Taking advantage of compact structure, manufacturing convenience, and superior fluid mixing that promotes heat transport, the helically coiled channels are widely applied for HX in various applications, including steam generators (El-Genk *et al.*, 2017).

The enhancement in helically coiled tube HX has been extensively investigated numerically and experimentally (Liaw *et al.*, 2020; Darzi *et al.*, 2021; Li *et al.*, 2017; Chang *et al.*, 2020; Cao *et al.*, 2021; Yang *et al.*, 2021; Naghibzadeh *et al.*, 2019; Omidi *et al.*, 2018; Ali and Sabharwall, 2021). Reported results have shown that the helically coiled tube HX induces secondary vortices by centrifugal force, ultimately enhancing heat transfer rates. The heat transfer and pressure losses in helically coiled tubes are highly dependent on the flow conditions, such as the Reynolds number (Re) and the coil geometry, which include the tube diameter (d_h), coil mean diameter (D), and coil pitch (P), as shown in Fig. 1. Helically coiled tube HXs have been proven to be more efficient and compact (e.g., large heat transfer area per unit volume) when compared to most traditional HXs (El-Genk and Schiener, 2017, Farnam *et al.*, 2021; Seara *et al.*, 2014). However, there is still a strong need to enhance the heat transfer performance and increase the compactness of the helical tube HX technology beyond the existing capabilities. Previously investigated passive performance enhancements for the helically coiled tube include adopting surface ribs and dimpled surfaces, wall corrugation, tube inserts for turbulence enhancements, tube cross-section modifications, and twisting (Kumar *et al.*, 2021; Chang *et al.*, 2020; Wang *et al.*, 2018; 2020; Sadeghianjahromi *et al.*, 2021; Cancan *et al.*, 2017; Zheng *et al.*, 2018; Zachàr *et al.*, 2010; Ali *et al.*, 2018; Hughes *et al.*, 2017)

Zheng *et al.* (2018) numerically evaluated the enhancements of dimpled helical coiled tubes to intensify the secondary flow and improve the heat transfer with the expense of a much higher pressure drop. Solanki *et al.* (2020) experimentally studied the pressure drop of dimpled helical coiled tubes using R-600a, discovering the average pressure drop of dimpled helical coiled tubes to be roughly 74-130% higher than smooth helical coiled tubes. The effects of adding internal ribs to the inner wall of helically coiled tubes were investigated by Li *et al.* (2017). The combination of augmented secondary flow and additional swirling enhanced the convective heat transfer. Kumar *et al.* (2021) investigated the heat transfer and pressure drop characteristics of micro-fin helically coiled tubes. The performance factor increased with an increase in fin numbers, showing an increase in Nu by 39-51% and 22-36% higher pressure drop than regular helical coil tube HX.

The effects of adding spherical corrugation to helically coiled tubes were investigated by Cancan *et al.* (2017). The corrugated tube was proven to provide significant eddy mixing and improve the heat transfer at the cost of higher pressure drop. Compared with smooth helically coiled tubes, the spherical corrugation provided 5-70% higher Nu and 1-

* *Corresponding Author Email: amirali@isu.edu*

Global Digital Central
ISSN: 2151-8629

24% higher friction factor (f). Darzi *et al.* (2021) evaluated the thermal performance of coiled tubes with a helical corrugated wall. The corrugated wall was concluded to significantly augment the heat transfer and thermal performance. Experiments of helically coiled wall corrugated tubes performed by Rainieri *et al.* (2012, 2013) showed that curvature and corrugation enhance the heat transfer with pressure drop penalties augmented to about 1-1.5 times. Zachár *et al.* (2010) added spherical corrugation to the outer side of the wall and a helical rib on the inner side of the wall to a helical tube configuration. Compared to a circular cross-sectional helical tube, the combination showed an 80-100% increase in heat transfer for the inner side and a 10-60% relative pressure drop increase. Cao *et al.* (2021) investigated a helical tube-in-tube heat exchanger with a corrugated inner tube and corrugated outer tube, showing the rate of corrugating the outer tube of the heat exchanger increases heat transfer is significantly enhanced when compared to only inner tube corrugation. Twisted tape inserts in circular cross-sectional helical tubes were investigated for both laminar and turbulent flow by Kurnia *et al.* (2020) and Liaw *et al.* (2020). The twisted tape was proven to enhance the secondary flow and heat transfer. For the laminar regime, the heat transfer performance was reported to be capable of enhancement up to four times compared to conventional tubes. Similar behavior was observed for turbulent flow.

Applying non-circular cross-sections to the helical configuration has been widely investigated. Naghibzadeh *et al.* (2019) investigated the heat transfer enhancement of a helical coil with a flattened cross-section, showing that the cross-section is more thermally effective than circular ones. Omidi *et al.* (2018) investigated the effects of lobed cross-sections on the heat transfer in helical coiled HXs, showing an increase in Nu and decrease in f as the number of lobes in the cross-section increases. In a helical configuration, Yang *et al.* (2021) investigated the heat transfer with several non-circular cross-sections: triangle, square, hexagon, octagon, decagon, and dodecagon. The flow and heat transfer rates in corner areas were weaker than in non-corner areas, showing that the heat transfer and pressure drop increase as the number of sides increases. Kurnia *et al.* (2016) numerically investigated the effects of various helical tube cross-sections on the heat transfer performance. Results showed that the helical tube configuration will always have higher heat transfer performance regardless of the cross-sections compared to straight tube counterparts. The square cross-section yielded the highest heat transfer performance but required the highest pressure drop, thus making it the least efficient cross-section.

Several analyses added twisting to non-circular cross-sectional helical tube configurations. Chang *et al.* (2020) investigated turbulent flow and heat transfer of helical coils with a twisted section using a square cross-section. Results showed that the swirl enhancement caused by the twisting dominated the Nu and f augmentation. Relative to the untwisted coil, the twisting of the square cross-section caused a 19% increase in Nu and a 69.8% increase in f. Farnam *et al.* (2021) further investigated the effects of helically twisted tubes with square cross-sections on single-phase forced convective heat transfer. The heat transfer performance was enhanced by applying twisting to the walls, enhancing Nu by about 14.2% and increasing f by about 7.7%. Trilobal cross-sectional helical tubes with a twist were experimentally and numerically investigated by Wang *et al.* (2020). Results showed that the trilobal cross-section geometry creates enhanced secondary flow beyond circular cross-sections, ultimately improving the heat transfer performance. The addition of twisting to the trilobal tube was also shown to significantly improve the heat transfer with the expense of higher pressure drop. The helical circular cross-section geometry had the lowest pressure drop, followed by the trilobal and twisted trilobal. Compared to the circular helical tube, the thermal performance of the twisted trilobal helical coiled tube increased by 19–31%.

The main objective is to continue investigating the impact of tube cross-section flow area combined with the twist effect in helical tube HX. The proposed study evaluates the performance of a new conceptual HX design that combines the helical coiled (Fig. 1a) geometry with an oval-twisted tube to form an oval-twisted helical tube configuration (Fig. 1b). Straight oval-twisted tube HXs have been implemented in industrial heat transfer applications for several decades. As reported in the literature, the heat transfer coefficient is higher for the straight tubes with oval twisting than for circular tubes with a slight increase in the pressure drop (Ali *et al.*, 2019). The combined swirl velocity provided by the oval-twisted geometry and induced secondary flow vortices by a helical shape would result in a higher transfer performance and a more compact HX than both individual technologies. The oval-twisted tubes reduce fouling due to fewer stagnation zones, resulting in lower pressure drop than other flow configurations (Wang *et al.*, 2020). The study evaluates key parameters, including the flow Reynolds number and coil curvature (tube to helical coil diameter ratio) for optimum performance under isothermal boundary conditions. Isothermal wall conditions practically exist when the HX experiences phase change (steam generator and condenser) on the outer surface of the tube (shell side). An additional advantage of the new helically coiled oval-twisted tube configuration is minimizing or eliminating dead flow zones and reducing the possibility of forming hot spots. Also, the new tube configuration reduces vibration and helps minimize or eliminate the need for support due to the tube's self-supporting nature (Hughes *et al.*, 2017).

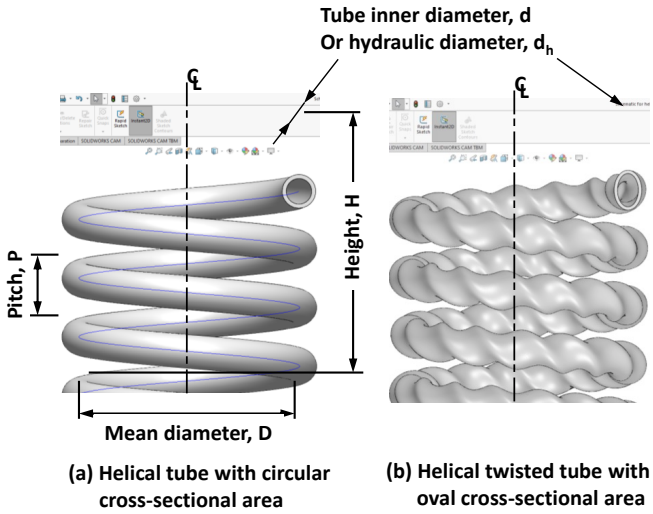

Fig. 1 Schematics of the helically (a) circular, (b) oval-twisted tubes.

2. NUMERICAL ANALYSIS

This study proposes a twisted helical coil with an oval cross-sectional flow area as a novel passive heat transfer enhancement for HX applications. The novel geometry takes advantage of enhanced heat transfer performance and large heat transfer area per unit volume provided by the combined oval-twisted and helical shapes (see Fig. 1b). The numerical study was conducted using the computational fluid dynamics (CFD) commercial package, Star-CCM+. The heat transfer and friction factor associated with laminar flow under isothermal wall conditions are presented. All results are compared with the helical coil with a circular cross-sectional flow area to quantify the enhancement provided by the new geometry. The effects of the curvature diameter ratio (d_h/D) on the thermal and hydrodynamic performances are presented.

2.1 Problem Statement and Boundary Conditions

Combining the oval-twist to the helical tube geometry to form an oval-twisted helical tube is a new channel concept, and no data is currently available in the literature to validate it. The objective was to evaluate the heat transfer enhancement by the generated swirl velocity component induced by the oval-twisted tube. The combined secondary flow induced by the helical shape and swirl velocity by the oval-twisted cross-section was expected to extend the heat transfer performance further than helical tubes with the circular cross-sectional flow area.

Global Digital Central
ISSN: 2151-8629

The circular helical tube diameter (d) or hydraulic diameter (d_h) for the oval-twisted helical tube, and the coil length (L) are kept constants for all cases to quantify the effect of coil geometry on the flow hydrodynamics and heat transfer. The number of coil turns and coil height (H) are dependent on the mean coil diameter (D). The helically twisted tube cross-section was elliptical, and the twist pitch (P) and aspect ratio (a/b: major axis of tube cross-section/minor axis of tube cross-section) were kept constant. The following table summarizes the geometrical and operating parameters investigated:

Table 1 Geometrical and operating parameters for the current study.

Parameter	Value	Units
Tube diameter or hydraulic diameter, d or d_h	17.44	mm
Coil mean diameter, D	75-225	mm
Oval-aspect ratio, a/b	2	
Coil pitch, P	40	mm
Coil height, H	113-336	mm
Coil length, L	2000	mm

The heat transfer coolant utilized in this numerical analysis was water. A constant fluid inlet temperature (T_{in}) of 300 K and an isothermal wall temperature (T_w) of 350 K were applied. The variation of fluid thermophysical properties with temperature may impact positively and negatively the calculated hydrodynamic and heat transfer parameters. For example, the bulk fluid would have a higher temperature, lower viscosity, and lower friction factor than what is calculated at the fluid inlet temperature. At this research stage, the authors decided to consider constant thermophysical properties to quantify a base case calculated Nu and f for better understanding and interpretation of the expected performance enhancement provided by the oval-twisted helical over the circular helical geometry. All constants' properties are quantified based on the flow inlet temperature, as observed in Table 2.

Table 2 Thermophysical properties of water evaluated at T_{in} = 300 K.

Thermophysical Property	Value	Units
Density, ρ	998.2	kg/m^3
Thermal conductivity, k	0.6	W/m·K
Dynamic viscosity, μ	0.001	Pa·s
Specific heat, Cp	4182	J/kg·K

The uniform inlet velocity was in the laminar flow regime for the Reynolds number (Re) range of 250-2000 for all geometrical configurations. The mean coil diameter (D) is used to calculate the flow Re and Dean number (De) for the helical coils:

$$Re = \frac{\rho u_i d_h}{\mu}, De = Re\sqrt{\frac{d_h}{D}} \quad (1)$$

The flow T_{in} and the bulk average fluid exit temperature (T_{ex}) are utilized to calculate the total thermal power removed (Q), the convective heat transfer coefficient (h_C), and the Nu.

$$Q = \dot{m}C_p(T_{ex} - T_{in}) \quad (2)$$

$$h_C = \frac{Q}{A_w \Delta T_{LMTD}} \quad (3)$$

$$Nu = \frac{h_C d_h}{k} \quad (4)$$

where $\dot{m}$ is the mass flow rate and A_w is the heat transfer surface area ($\pi d_h L$). The Logarithmic Mean Temperature Difference, ΔT_{LMTD} is calculated as:

$$\Delta T_{LMTD} = \frac{(T_w - T_{in}) - (T_w - T_{ex})}{ln\left(\frac{T_w - T_{in}}{T_w - T_{ex}}\right)} \quad (5)$$

Finally, the f is calculated using the following equations:

$$f = \frac{\Delta P}{\frac{L\rho u_i^2}{2d_h}} \quad (6)$$

where ΔP is the pressure drop (Pa).

2.2 Mech Sensitivity Study

The independence of the numerical results of the mesh element refinement is an essential aspect of the numerical analysis. In addition, the near-wall region is vital to consider for the investigated helical and oval-twisted geometries. These two parameters are crucial to accurately capture the temperature and velocity gradients near the wall to predict hydrodynamic and thermal behavior. The polyhedral mesh was adopted to generate the volume mesh. The applied mesh and prism layers for the oval-twisted and circular helical coils are partially shown in Fig. 2.

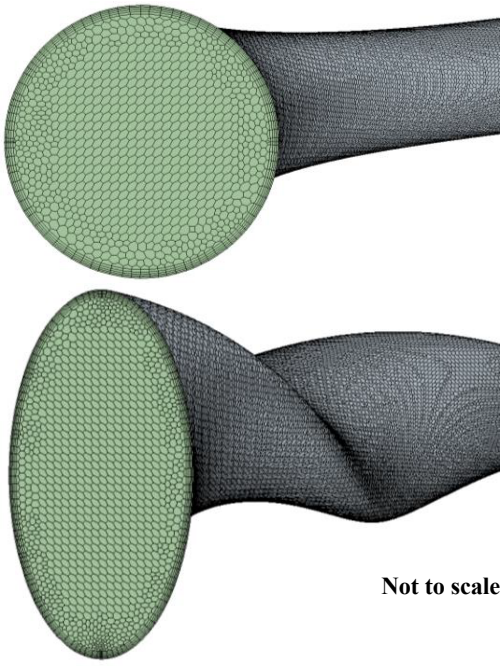

Fig. 2 Computational mesh for circular and oval cross-sections with prism layers near the wall.

The mesh sensitivity on the Nu and ΔP for circular and oval-twisted helical coils was quantified using the relative error method. The calculated Nu and ΔP were compared for five different mesh sizes with increasing refinements: (1) very coarse; (2) coarse; (3) regular; (4) fine; and (5) finer mesh. The total mesh element and corresponding relative error for Re = 500 are presented in Table 3. The relative errors are calculated using the finer mesh data as the reference (baseline) case:

$$R_{Nu} = \frac{Nu - Nu_{baseline}}{Nu_{baseline}}, R_{\Delta P} = \frac{\Delta P - \Delta P_{baseline}}{\Delta P_{baseline}}. \quad (7)$$

The mesh sensitivity analysis was also extended to Re = 2000. The relative errors are less than 3% and 2.3% for Nu and ΔP, respectively. Therefore, the fine-mesh size (e.g., 2,305,224 elements) was sufficient for the cases of circular and oval-twisted helical tubes.

Table 3 Relative errors in the calculated Nu and ΔP

Mesh	Elements (million)	Re = 500			
		Nu	R_{Nu}(%)	ΔP(Pa)	$R_{\Delta P}$ (%)
Coarser	~ 0.5	6.55	1.18%	3.21	0.45%
Coarse	~ 1.0	6.51	0.55%	3.22	0.08%
Normal	~ 1.5	6.49	0.24%	3.23	0.08%
Fine	~ 2.3	6.48	0.12%	3.22	0.08%
Finer	~2.9	6.47	Base	3.22	Base

2.3 Model Selection

Multiple numerical models were investigated to ensure the calculation accuracy for different tube geometries within the range of low Re (e.g., 250–2000). Though the flow is laminar, the swirling flow induced by the oval-twisted geometry may result in a higher flow mixing, and a turbulence model would provide accurate results. The low Reynolds k-ε model was also considered for capturing accurate hydrodynamic and heat transport gradients within the viscous layer near the wall at low Re as recommended for close geometries (Cheng *et al.*., 2017). The accuracy of the numerical models was verified by comparing the calculated Nu and f to data from the literature (Fig. 3). The Low Reynolds k-ε and laminar flow models were applied to helical tubes over the range of Re = 250-2000 (De = 85-682). The base case, circular-helical tube (d_h/D = 0.12) Nu results were compared to Rainieri *et al.*, 2012 (Eqn. 8) and Manlapaz and Churchill, 1981 (Eqn. 9), and the f results were compared to White, C. M., 1929 (Eqn. 10) for validation. As shown in Fig. 3a, the Low Reynolds k-ε Nu results show almost perfect agreement, while the laminar flow model shows Nu within 10% agreement with Eqns. 8, and 9. Both Low Reynolds k-ε and laminar flow models show consistent results for the f within 4% agreement with Eqn. 10, as shown in Fig. 3b.

$$Nu = 1.168De^{0.47}Pr^{0.16} \tag{8}$$

$$Nu = \left[\left(3.657 + \frac{4.343}{X_1}\right)^3 + 1.158\left(\frac{De}{X_2}\right)^{3/2}\right]^{1/3} \tag{9}$$

$$X_1 = \left(1 + \frac{957}{De^2\,Pr}\right)^2,\ X_2 = 1 + \frac{0.477}{Pr}$$

$$f = f_s\left[1 - \left(1 - \left(\frac{11.6}{De}\right)^{0.45}\right)^{1/0.45}\right]^{-1} \tag{10}$$

The overall Nu and f results presented for the base case using the Low Reynolds k-ε model slightly outperformed the laminar flow model. Thus, the Low Reynolds k-ε model was selected for further numerical analyses.

3. RESULTS ANALYSIS

A baseline case (d_h/D = 0.12) was made to compare circular and oval-twisted helical tubes Nu and f results, using the fine mesh and applied the Low Reynolds k-ε model for all cases. All investigated tubes for the concept proof are identical and exhibit the same flow (Re = 250-2000) and boundary conditions (T_{in} = 300 K and T_w = 350 K). The baseline case results presented in Fig. 4 show that the swirling velocity provided by the oval-twisting enhances the heat transfer performance (Fig. 4a) and increases pressure drop (Fig. 4b) compared to the circular helical tube. The results presented in Fig. 4 indicate that combining the oval-twisted and helical geometries would highly intensify the Nu and increase the ΔP over the circular helical tube. The impact of curvature ratio d_h/D was investigated to optimize the geometrical parameters on the heat transfer and pressure drop performance.

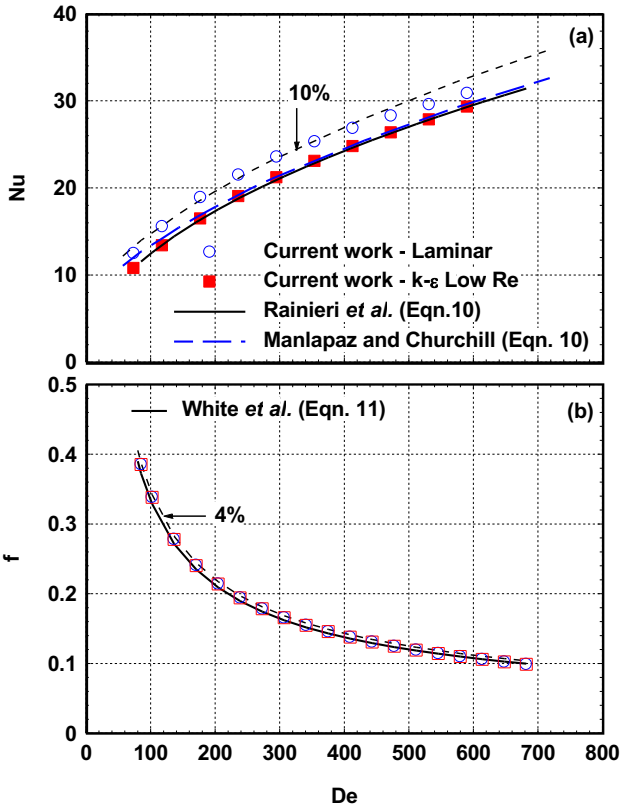

Fig. 3 Comparison of the Nu and f for laminar and k-ε solvers with models from the literature.

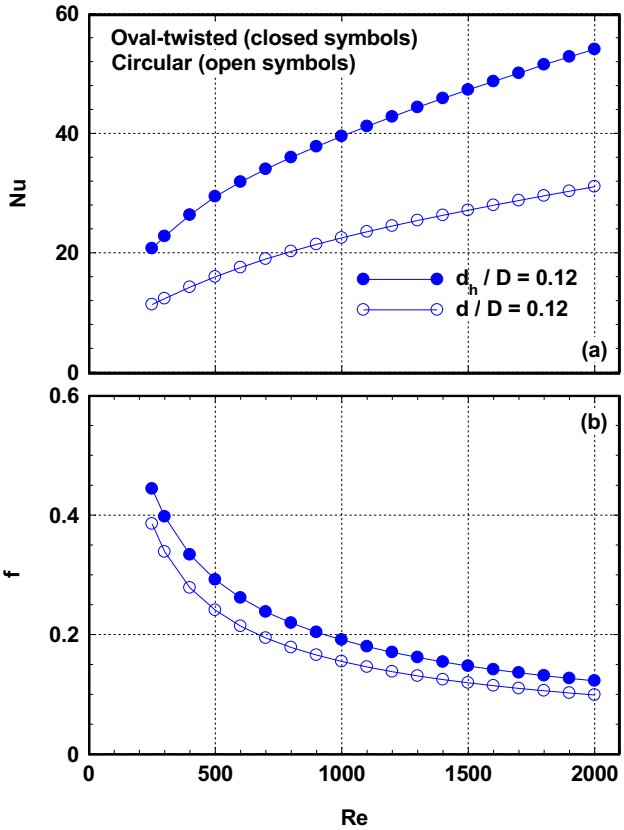

Fig. 4 Comparison of the Nu and f for laminar flow in oval-twisted and circular helical tubes for the base case (d_h/D = 0.12)

Global Digital Central
ISSN: 2151-8629

3.1 Effects of Coil Curvature

The effects of the coil curvature, d_h/D, for the circular helical tubes and oval-twisted helical tubes on the heat transfer performance, is shown in Fig. 5a and 5b, respectively. As the coil mean diameter decreases, the coil curvature increases, and Nu is shown to increase for a given Re. The centrifugal force generated by a smaller coil diameter enhances heat transfer performance than the larger one, resulting in a more significant velocity gradient and induced secondary flow. The induced secondary flow increases with increasing Re, as shown in Fig. 5a.

The enhancement becomes more recognized for the oval-twisted helical coil, as shown in Fig. 5b. The twist geometry strengthens the swirling flow, and the helical shape induces secondary flow, explaining the higher heat transfer performance between the two geometries for a given Re. Figure 6 presents the vorticity induced by the circular helical tube (top) versus the oval-twisted helical tube (bottom) at different Re measured at the midpoint of the coil length for a d_h/D of 0.12 over the investigated range of Re. The combined geometries result in higher vorticity over the circular helical tube. The vorticity increases as the Re increases for both geometries, but the oval-twisted helical tube always provides a higher vorticity magnitude at any given Re, justifying the increased Nu for the combined geometry.

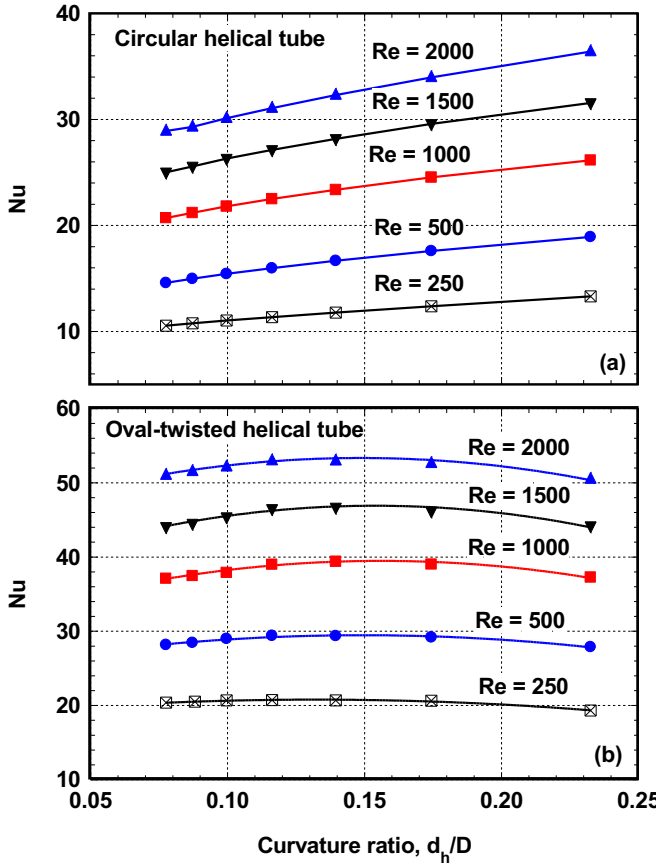

Fig. 5 Effect of coil curvature diameter ratio (d_h/D) on Nu

The performance curves comparing the Nu and f between the circular and oval-twisted helical tubes for different curvature ratios over the range of laminar flow Re under isothermal wall conditions are presented to quantify the overall performance Fig. 7. The open symbols in Figs. 7a and 7b are for circular helical geometry, and the closed symbols are for oval-twisted helical geometry. The comparison clearly shows that the oval-twisted provides higher Nu at a given Re (Fig. 7a). As the flow velocity increases (higher Re), the induced vorticity increases (Fig. 6), resulting in increased Nu. The increased vorticity also results in higher f for all cases investigated.

Unlike circular helical tubes, the oval-twisted helical geometry shows a peak performance at a coil curvature of 0.17, as shown in Fig. 7a. For a $d_h/D > 0.17$, the centrifugal force becomes dominant and reduces the enhancement provided by the swirling velocity, causing the overall heat transfer performance to decrease but remain higher than those determined for the circular helical tubes. At lower values of coil curvature, the oval-twisted helical tubes experience higher pressure drop than circular helical tubes. As the coil curvature increases, the reduced swirling velocity contribution results in decreasing pressure drop, and the friction factor for the oval-twisted helical tube approaches the friction factor of the circular helical tube at higher heat transfer performance (Fig. 7a and 7b).

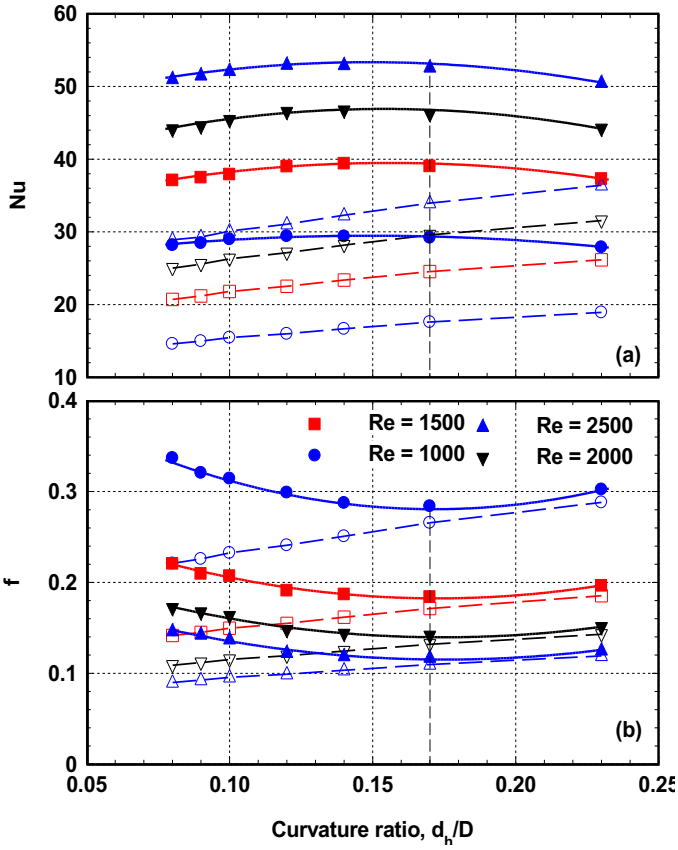

Fig. 7 Performance comparison of circular and oval-twisted helical tube geometries with varying d_h/D.

3.2 Enhancement and Performance Factor

The effectiveness of the heat transfer enhancement can be evaluated by the thermal performance factor (η), which presents the relative change in the heat transfer rate to the relative change in the friction factor, as provided by equation 11.

$$\eta = (\frac{Nu}{Nu_o})/(\frac{f}{f_o}) \quad (11)$$

The thermal performance factor of the oval-twisted helical geometry over the circular helical geometry is presented in Fig. 8. As shown in Fig. 8, the performance factor peaks at the curvature ratio at which the Nu reaches its maximum value (see Fig. 7a) and the f reaches its minimum value (see Fig. 7b) over the range of Re. As the Re increases, the relative increase in the Nu is less than the relative increase in the f for the oval-twisted helical geometry over the circular helical geometry, resulting in a decrease in the thermal performance factor. Figure 8 indicates that the performance factor decreases as the Re increases.

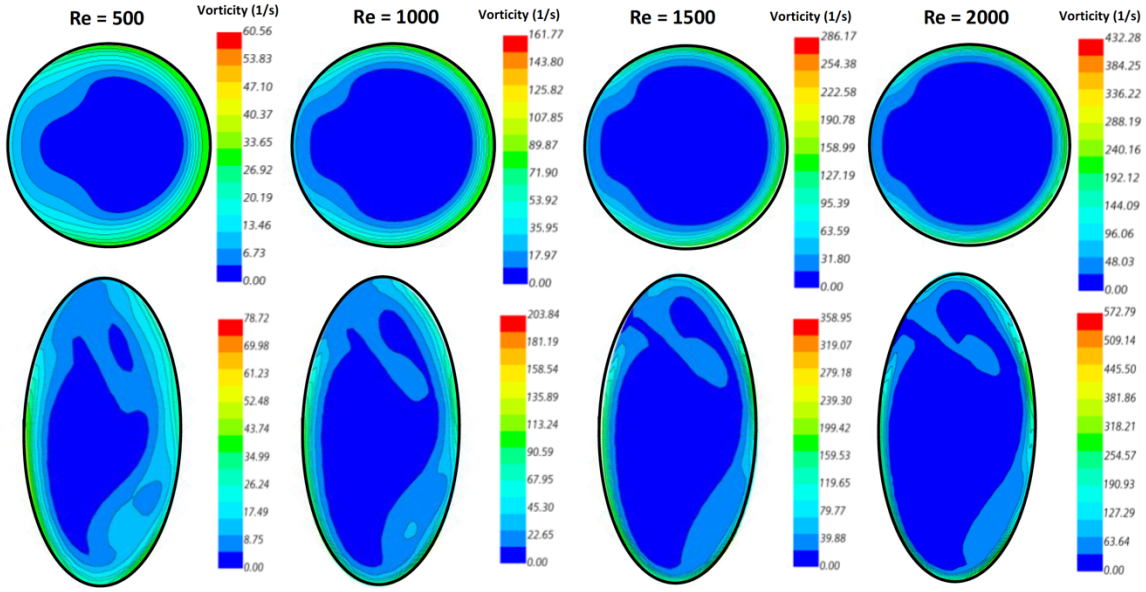

Fig. 6 Comparison of the induced vorticity for circular and oval-twisted helical flow tube channels (base case).

3.3 Performance Correlations

A practical method to present the heat transfer performance of newly developed flow channel geometry is developing correlations for the Nu and the f. These correlations facilitate the comparison with other existing data in the literature. In addition, the correlations can be implemented in additional computational tools for further analyses, including thermal stress and induced flow vibration. Helically coiled tubes of different cross-sectional flow areas are presented in the literature in the general form:

$$Nu = A \cdot De^{B} Pr^{C} \tag{12}$$

The friction factor for helical coils of variant cross-sectional flow areas can be expressed as a ratio of the Darcy friction factor in the form:

$$\frac{f}{f_c} = A \cdot Re^{B} \left(\frac{d_h}{D}\right)^{C} \tag{13}$$

where A, B, and C are constants.

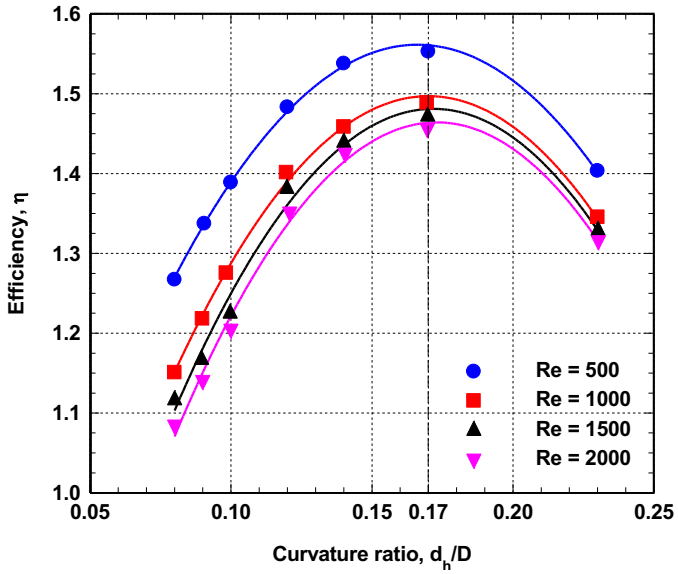

Fig. 8 The thermal performance efficiency of the oval-twisted helical tube for various Re and, d_h/D.

The current Nu numerical data presented in Fig. 9a for the circular helical tube are in high agreement with the correlation from Rainieri et al., 2012 (Eqn. 8). A similar formula is proposed for the oval-twisted helical tube in the form:

$$Nu = \psi De^{0.47} Pr^{0.16} \tag{14}$$

$$\psi = 2.36 - 2.08\left(\frac{d_h}{D}\right) - 3.92\left(\frac{d_h}{D}\right)^2$$

where ψ is a nonlinear function reflecting the peak performance archived at d_h/D = 0.17.

As shown in Fig. 9a, the proposed correlation for the Nu is in good agreement within ± 6% with the numerical data. In a similar approach, the current f numerical data is presented in Fig. 9b. The calculated friction factor agrees with the general form of the helical coil friction factor, as observed in equation 13. A similar formula is proposed for the oval-twisted helical tube in the form:

$$f = \lambda\, Re^{0.36} \left(\frac{d_h}{D}\right)^{0.16} \tag{15}$$

$$\lambda = 0.421 - 2.14\left(\frac{d_h}{D}\right) - 6.16\left(\frac{d_h}{D}\right)^2$$

where λ is a nonlinear function reflecting the minimum f archived at d_h/D = 0.17.

As shown in Fig. 9b, the proposed correlation for the f and the numerical data are in good agreement within ± 5%.

4. SUMMARY and CONCLUSION

A new heat transfer enhancing geometrical configuration combining the effects of oval-twisted and helical tube geometries was numerically investigated for their heat transfer and hydrodynamic performances. The concept integrates the swirling velocity induced by the oval-twisting and the centrifugal force from the helical shape to strengthen the secondary flow and enhance heat transfer performance. The contribution of the helical and oval-twisted shapes was quantified in a study that investigated Nu and f of helical tubes with circular cross-sectional flow areas and straight tubes with oval-twisted cross-sectional flow areas under the same geometrical, operating, and boundary conditions.

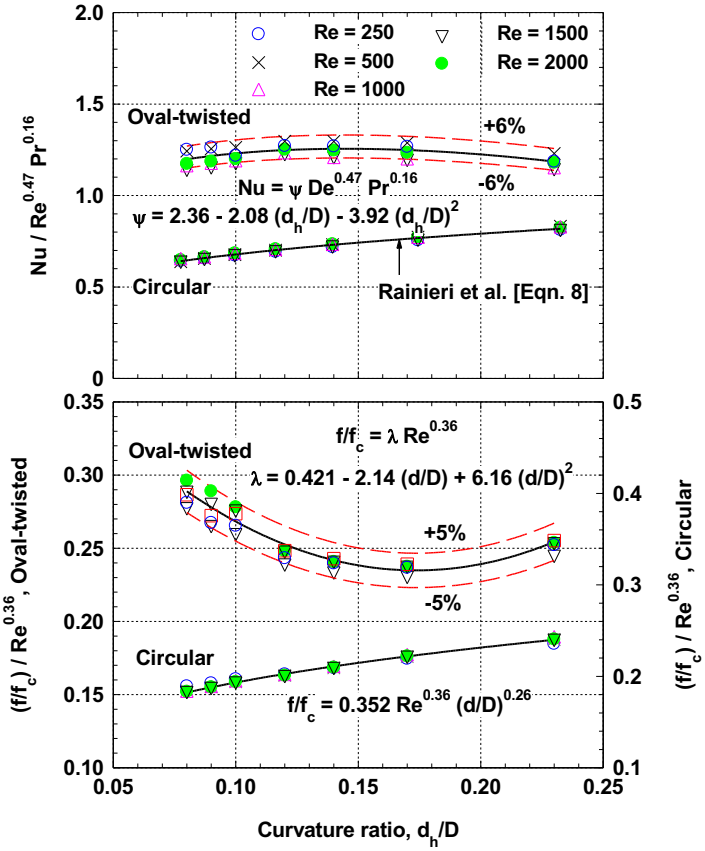

Fig. 9 Development of Nu correlations and deviation from the numerical results

The numerical analysis was conducted to demonstrate: (1) the improved heat transfer capabilities of the oval-twisted helical tube compared with the previously established helical tube for advanced HX design; (2) the impacts of changing the mean coil diameter for oval-twisted helical tubes on the heat transfer and hydrodynamic performances; and (3) the development of Nu and f correlations for the oval-twisted helical tube.

The oval-twisted helical coil showed higher heat transfer performance than the helical coil with a circular cross-section (Fig. 5). The oval-tube twist-induced vorticity and the secondary flow induced by the helical geometry contributed significantly to enhancing heat transfer performance over the circular helical tube configuration (Fig. 6). These results formed the motivation to add the oval-twisted flow cross-section to the helical tube for optimum performance. Under the same flow and boundary conditions, the oval-twisted helical tube has been shown to increase the Nu over the helical tube with a circular cross-sectional flow area with the expense of a higher f (Figs. 6 and 7). The effects of tube diameter curvature ratio (e.g., tube to coil mean diameter, d_h/D) on the heat transfer and hydrodynamic performance was presented. The oval-twisted helical tube has been shown to increase the Nu over the helical tube with a circular cross-sectional flow area at the expense of a higher f. The Nu and f increased linearly with d_h/D for the circular helical tube and parabolic for the oval-twisted helical tube, with the highest Nu and lowest f occurring at d_h/D = 0.17 (Fig. 7). The enhancement performance factor (η) ranges between 46–56% for the oval-twisted over the circular helical tubes (Fig. 8). The Nu and f correlations presented for the oval-twisted helical tube (equations 14 and 15) show good agreement with the numerical results; ± 6% and ± 5% for the Nu and f, respectively.

ACKNOWLEDGEMENTS

The Idaho State University and Center of Advanced Energy Studies sponsored and funded this research through ISU-CAES small grant funding program. This research used the High-Performance Computing Center resources at Idaho National Laboratory, supported by the Office of Nuclear Energy of the US Department of Energy and a Nuclear Science User Facility.

NOMENCLATURE

A, B, C	constants for equations 13 and 14
A, b	oval minor and major diameters (m)
a/b	oval aspect ratio
A_s	heat transfer surface area (m^2)
CFD	computational Fluid Dynamics
Cp	specific heat (J/kg·K)
D	coil mean diameter (m)
De	Dean number, $Re\sqrt{d_h/D}$
De_m	modified Dean number, $De^{0.86}\delta^{0.09}(d/D)^{-0.38}$
d, d_h	tube inner or hydraulic diameter (m)
d/D	tube diameter curvature ratio
f	friction factor or coefficient
f_s	Darcy friction factor coefficient
H	coil height (m)
HX	heat exchanger
h_C	convection heat transfer coefficient (W/m^2·K)
k	thermal conductivity (W/m·K)
L	tube or coil length (m)
$\dot{m}$	mass flow rate (kg/s)
Nu	Nusselt number
P	coil pitch (m)
Pr	Prandtl number
Q	thermal power (W)
Re	Reynolds number
R_{Nu}	relative numerical error for Nu
$R_{\Delta P}$	relative numerical error for ΔP
T	temperature (K)
u	mean velocity (m/s)

Greek Symbols

δ	coil curvature
ΔP	pressure drop (Pa)
ΔT	temperature difference (K)
ρ	density (kg/m^3)
μ	dynamic viscosity (Pa·s)

Subscript

ex	exit
i, in	inlet
$LMTD$	Logarithmic Mean Temperature Difference
o	circular cross-section
w	wall

REFERENCES

Amir, A., Bryan, W., and Edward, B., 2019, "Triple flow heat transfer with intermediate oval-twisted tube for FHRs," *18th International Topical Meeting on Nuclear Reactor Thermal Hydraulics* (**NURETH-18**), Portland, Oregon, USA.

Amir, A., Piyush, S., 2021, "In-Plane Oval-Twisted Spiral Tube Heat Exchanger for Nuclear Applications," *American Nuclear Society (ANS) Annual Meeting,* Virtual meeting.

Cancan, Z., W. Dingbiao, X. Sa, H. Yong, and P. Xu, 2017, "Numerical investigation of heat transfer and pressure drop in a helically coiled tube with spherical corrugation, "*Int. J. Heat Mass Transfer*, **113**. https://doi.org/10.1016/j.ijheatmasstransfer.2017.05.108

Cao, Y., Ayed, H., Anqi, A.E., Tutunchian, O., Dizaji, H.S., Pourhedayat, S., 2021, "Helical tube-in-tube heat exchanger with a corrugated inner tube and corrugated outer tube; experimental and numerical study," *Int. Journal of Thermal Science*, **170**. https://doi.org/10.1016/j.ijthermalsci.2021.107139

Chang, S.W., Wu, P.-S., Cai, W.L., Liu, J.H., 2020, "Turbulent flow and heat transfer of helical coils with twisted section," *Applied Thermal Engineering*, **180**. https://doi.org/10.1016/j.applthermaleng.2020.115919

Cheng, J., Z. Qian, and Q. Wang, 2017, "Analysis of heat transfer and flow resistance of twisted oval tube in low Reynolds number flow," *Int. J. Heat Mass Trans.*, **109**. https://doi.org/10.1016/j.ijheatmasstransfer.2017.02.061

Darzi, A. A. R., Abuzadeh, M., Omidi, M., 2021, "Numerical investigation on the thermal performance of coiled tube with a helical corrugated wall," *Int. Journal of Thermal Science*, **161**. https://doi.org/10.1016/j.ijthermalsci.2020.106759

El-Genk, M. S., and T.M. Schriener, 2017, "A review and correlations for convection heat transfer and pressure losses in toroidal and helically coiled tubes," *Heat Transfer Engineering*, **38**. https://doi.org/10.1080/01457632.2016.1194693

Farnam, M., Khoshvaght-Aliabadi, M., Asadollahzadeh, M.J., 2021, "Intensified single-phase forced convective heat transfer with a helical-twisted tube in coil heat exchangers, "*Annals of Nuclear Energy*, **154**. https://doi.org/10.1016/j.anucene.2020.108108

Ghobadi, M., and Y. S. Muzychka, 2016, "A review of heat transfer and pressure drop correlations for laminar flow in curved circular ducts," *Heat Transfer Eng.*, **37**. https://doi.org/10.1080/01457632.2015.1089735

Hughes, J. T., 2017, "Experimental and computational investigations of heat transfer systems in fluoride salt-cooled high-temperature reactors," *Ph.D. dissertation*, University of New Mexico (UNM), USA. https://doi.org/10.2172/1562302

Kumar, E. P., Solanki, A. K., Kumar, M. M. J., 2021, "Numerical investigation of heat transfer and pressure drop characteristics in the micro-fin helically coiled tubes, "*Applied Thermal Engineering*, **182**. https://doi.org/10.1016/j.applthermaleng.2020.116093

Kurnia, J. C., A. P. Sasmito, T. Shamim, and A. S. Mujumdar, 2016, "Numerical investigation of heat transfer and entropy generation of laminar flow in helical tubes with various cross-sections," *Appl. Therm. Eng.*, **102**, 849–860. https://doi.org/10.1016/j.applthermaleng.2016.04.037

Kurnia, J. C., Chaedir, B. A., Sasmito, A. P., 2020, "Laminar convective heat transfer in a helical tube with twisted tape insert, "*Int. J. Heat and Mass Transfer,* **150**. https://doi.org/10.1016/j.ijheatmasstransfer.2020.119309

Li, Z., Zhai, Y., Bi, D., Li, K., Wang, H., Lu, J., 2017, "Orientation effect in helical coils with a smooth and rib-roughened wall: Toward improved gas heaters for supercritical carbon dioxide Rankine cycles, "*Energy* **140**. https://doi.org/10.1016/j.energy.2017.09.010

Liaw, K. L., Kurnia, J. C., Sasmito, A. P., 2020, "Turbulent convective heat transfer in a helical tube with twisted tape insert, "*Int. J. Heat and Mass Transfer,* **169**. https://doi.org/10.1016/j.ijheatmasstransfer.2021.120918

Manlapaz, R. L., and Churchill, S. W., 1981, "Fully Developed Laminar Convection from a Helical Coil, "*Chemical Engineering Communications*, **9**, 185–200. https://doi.org/10.1080/00986448108911023

Naghibzadeh, S.K., Hajmohammadi, M.R., Saffar-Avval, M., 2019, "Heat transfer enhancement on a nanofluid in a helical coil with flattened cross-section," *Chem Eng. Research and Design*, **146**, 36-47. https://doi.org/10.1016/j.cherd.2019.03.008

Omidi, M., Farhadi, M., Darzi, AAR, 2018, "Numerical study of heat transfer on using lobed cross-sections in helically coiled heat exchangers: Effect of physical and geometrical parameters, "*Energy Conversion and Management*, **176**, 236-245. https://doi.org/10.1016/j.enconman.2018.09.034

Rainieri, S., Bozzoli, F., and Pagliarini, G., 2012, "Experimental Investigation on the Convective Heat Transfer in Straight and Coiled Corrugated Tubes for Highly Viscous Fluids: Preliminary Results," *International Journal of Heat and Mass Transfer*, **55**, 498–504. https://doi.org/10.1016/j.ijheatmasstransfer.2011.08.030

Rainieri, S., Bozzoli, F., Gattani, L., and Pagliarini, G., 2013," Compound Convective Heat Transfer Enhancement in Helically Coiled Wall Corrugated Tubes," *International of Journal Heat and Mass Transfer*, **59**, 353–362. https://doi.org/10.1016/j.ijheatmasstransfer.2012.12.037

Sadeghianjahromi, A., and C.-C. Wang, 2021, "Heat transfer enhancement in fin-and-tube heat exchangers: A review on different mechanisms, "*Journal of Renewable and Sustainable Energy*, **137**. https://doi.org/10.1016/j.rser.2020.110470

Seara, J. F., C. P. Pontevedra, and J. A. Dopazo, 2014, "On the performance of a vertical helical coil heat exchanger: Numerical model and experimental validation, "*Appl. Therm. Eng*. **62** (2). https://doi.org/10.1016/j.applthermaleng.2013.09.054

Solanki, A. K., and R. Kumar, 2020, "Condensation frictional pressure drop characteristic of R-600a inside the horizontal smooth and dimpled helical coiled tube in shell type heat exchanger," *Int. J. Therm. Sci.*, **154**. https://doi.org/10.1016/j.ijthermalsci.2020.106406

Wang, G., T. Dbouk, D. Wang, Y. Pei, X. Peng, H. Yuan, and S. Xiang, 2020, "Experimental and numerical investigation on hydraulic and thermal performance in the tube-side of helically coiled-twisted trilobal tube heat exchanger, "*Int. J. Therm. Sci.*, **153**. https://doi.org/10.1016/j.ijthermalsci.2020.106328

Wang, M., M. Zheng, M. Chao, J. Yu, X. Zhang, and L. Tian, 2018, "Experimental and CFD estimate a single-phase heat transfer in helically coiled tubes," *Progress in Nuclear Energy*, **112**, 185-190. https://doi.org/10.1016/j.pnucene.2018.12.015

White, C. M., 1929, "Fluid Friction and Its Relation to Heat Transfer, "*Transactions of Institution of Chemical Engineering*, **10**, 66–86.

Yang, M., Li, G., Liao, F., Li, J., Zhou, X., 2021, "Numerical study of the characteristic influence on heat transfer of supercritical CO_2 in a helically coiled tube with non-circular cross-section, "*Int. J. Heat. Mass. Transf.*, **176**. https://doi.org/10.1016/j.ijheatmasstransfer.2021.121511

Zachàr, A., 2010, "Analysis of coiled-tube heat exchangers to improve heat transfer rate with a spirally corrugated wall," *Int. J. Heat Mass Trans.*, **53**, 3928-3939. https://doi.org/10.1016/j.ijheatmasstransfer.2010.05.011

Zheng, L., Y. Xie, and D. Zhang, 2018, "Numerical investigation on heat transfer and flow characteristics in helically coiled mini-tubes equipped with dimples, "*Int. J. Heat Mass Transfer*, **126B**, 544-570. https://doi.org/10.1016/j.ijheatmasstransfer.2018.05.111